Kinetics of NiO Reduction and Morphological Changes in Composite Anodes of Solid Oxide Fuel Cells: Estimate Using Raman Scattering Technique[1]

D. A. Agarkov*, I. N. Burmistrov, F. M. Tsybrov, I. I. Tartakovskii, V. V. Kharton, and S. I. Bredikhin

Institute of Solid State Physics, Russian Academy of Sciences,
ul Akademika Osip'yana 2, 142432 Chernogolovka, Moscow oblast, Russia
*e-mail: agarkov@issp.ac.ru
Received July 17, 2015

Abstract—The kinetics of nickel reduction and morphological changes in Ni-10Sc1CeSZ composite anodes in medium–temperature solid oxide fuel cells (SOFC) are studied using the Raman spectroscopy technique with the help of application of optically transparent single crystal solid electrolyte membranes and also the thermogravimetric analysis technique. It is shown that the first reduction cycle differs considerably from all the further ones, which is related to morphological changes of nickel grains occurring during the first reduction cycle. A general scheme of occurrence of the process is suggested in studies of model cells using the Raman spectroscopy technique and also in the case of thermogravimetric analysis of powders; it explains the causes for significant differences between the total duration of the process as measured using different techniques. The results of the work can be used for optimization of the mode of initial reduction of the anodic SOFC electrode.

INTRODUCTION

Solid oxide fuel cells (SOFC) are promising electrochemical generators that directly convert chemical energy of fuel to electric and heat energy. It is necessary to decrease the working cell temperature to enhance the life cycle of SOFC–based power generators [1–3]. A decrease in the SOFC operating temperature to 500–800°C requires new electrode materials providing efficient operation in the given temperature range. Promising electrode materials for medium–temperature SOFC are materials of the lanthanum–strontium cobaltite–ferrite (LSCF) family [4–6]. They preserve high conductivity values, they are stable in contact with the solid electrolyte materials and also have a thermal expansion coefficient that is close to that of these materials. Meanwhile, the conventional anode material based on Ni-YSZ (92 mol % ZrO_2+8 mol % Y_2O_3) cermet [7–9] remains one of the most probable variants also in the case of a decrease in the SOFC operating temperature, as conductivity of the other known anodic materials is much lower; besides, they still contain additives based on metals, such as nickel and iron [10–12].

In the case of medium–temperature SOFC, it is important to study the kinetics of initial reduction of the anodic electrode when the cell reaches the operating mode, as this process can occupy significant time at low temperatures, up to tens of hours. This work provides estimates for the kinetics of reduction of the anodic electrode at the temperature of 500°C using the in situ Raman spectroscopy technique and also thermogravimetric analysis performed in a reducing atmosphere.

EXPERIMENTAL

The setup for in situ studies of electrode processes using the Raman scattering technique was described in detail earlier in [13]. The general scheme is presented in Fig. 1.

The setup consists of a gas–temperature test bench providing the control of the working temperature and gas mixture composition, a special sample holder, and also an optical scheme for registration of optical radiation in studies using the Raman spectroscopy technique.

---

[1] Published on the basis of the materials of III All-Russia Conference "Fuel Cells and Power Plants on Their Basis", Chernogolovka, 2015.
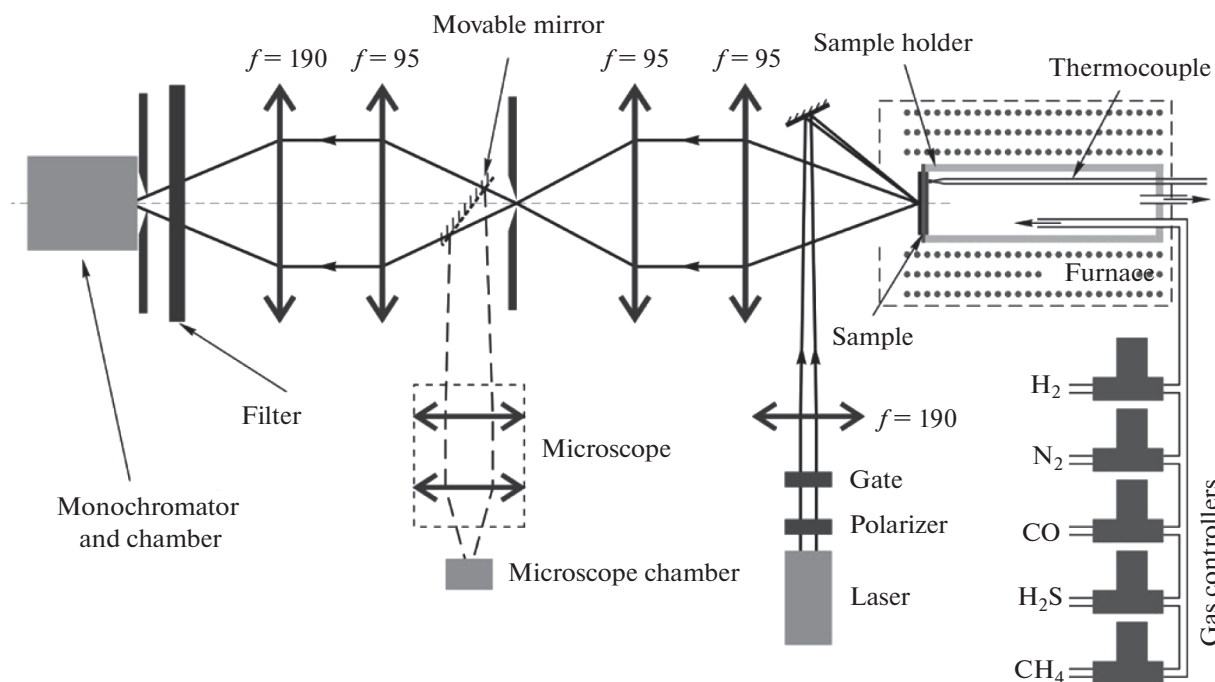
Fig. 1. Scheme of the research setup for in situ studies of electrode processes using the Raman scattering technique.

The gas–temperature testing bench consists of gas flow controllers (Bronkhorst, Netherlands) and also a high–temperature furnace manufactured in Institute of Solid State Physics, Russian Academy of Sciences. The gas system supplies hydrogen, nitrogen, carbon monoxide, hydrogen sulfide, and methane into the fuel chamber with the maximum flow of each component being 100 mL/min. The high–temperature furnace provides the operating temperature control to 1000°C and the heating rate of up to 400°C/h.

A special holder for samples represents a tube of single crystal sapphire. The sample is fixed on its face using sealing glass and also a spring mechanical holdback. Platinum wires are fixed on the tube for measurements using the two–electrode four–contact method, same as two thermal couples for temperature control within the fuel chamber and also outside the tube in close vicinity to the sample.

The optical system consists of a laser pumping subsystem based on laser focused by a collecting lens with the power of 30 mW and wavelength of 532 nm and also a system of scattered radiation registration. The registration system is based on a couple of collecting lenses focusing the image of the region of interest on the sample on the crossed optical gap to transmit to a CCD camera fixed on an optical microscope using a movable mirror. When the movable mirror is removed, the image of the region of interest is transmitted using the second couple of collecting lenses to the optical gap of the MDR-12 monochromator (Lomo, Russia)

with the further registration using a CCD camera (Princeton Instruments, USA).

SOFC samples for electrochemical studies were manufactured on the basis of single crystal membranes with the composition of 10Sc1YSZ (89 mol % ZrO_2 + 10 mol % Sc_2O_3 + 1 mol % Y_2O_3) produced by Institute of Physics, Russian Academy of Sciences [14, 15]. Solid electrolyte crystals were manufactured using the high–frequency heating technique in a cold crucible. Further, they were used to manufacture disks with the diameter of 21 mm and thickness of 250 and 500 μm in Institute of Solid State Physics, Russian Academy of Sciences. Studies of electric properties of single crystal membranes were reported earlier [16]. At 850°C, ionic conductivity of membranes exceeds 0.12 S/cm, which guarantees the quality of SOFC manufactured on their basis.

The anodic electrode was applied onto solid electrolyte membranes using the screen printing technique [17]. Nickel oxide powder (Sigma Aldrich, USA) was used as the initial compound. The results of works on optimization of preliminary preparation of nickel oxides for the manufacturing of composite SOFC anodes were published earlier [18]. According to the results of these works, the powder was subjected to preannealing at the temperature of 650°C for dehydration and removal of hyperstoichiometric oxygen from the amorphous particle shell with the "core–shell" microstructure. After this, the powder was mixed with the anion conductor of 10Sc1CeSZ (89 mol % ZrO_2+10 mol % Sc_2O_3+1 mol % CeO_2) (DKKK,
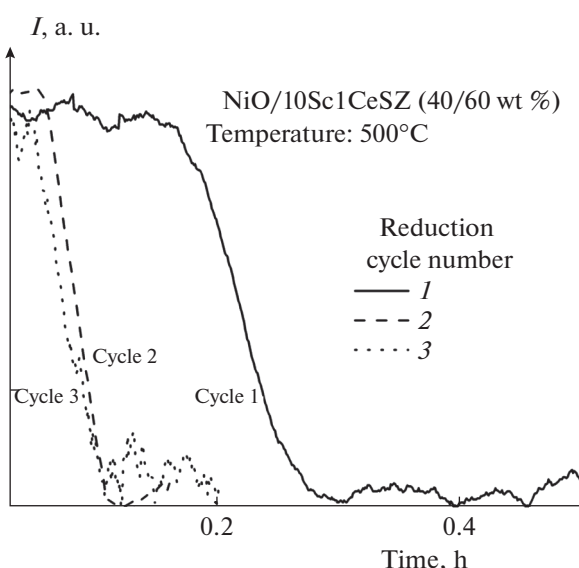
Fig. 2. Dependence of the intensity of the 615 cm^{-1} band in the Raman spectrum on time in the course of the anodic electrode reduction cycles.

Japan) at the ratio of NiO/10Sc1CeSZ = 40/60 wt %. The sample was subjected to grinding in a zirconium cup of a Fritsch Pulverisette 5 classic line planetary mill (Fritsch, Germany) using zirconium balls with the diameter of 3 mm. The grinding medium was a toluene/butanol/diethyladipate mixture with the volume ratio of 70/30/2 with addition of diaminopropane as a surfactant at the amount of 3% of the powder mixture mass. After milling, the powder mixture was dried at the temperature of 130°C and was mixed with a Heraeus V006-A two−component organic binder (Heraeus, Germany) at the ratio of 1 : 0.4. The dry substance/binder ratio was optimized before [19]. The obtained paste was applied onto membranes using the screen printing technique with the help of a Ekra Mat S45 machine (Ekra, Germany) through screens with the weaving density of 32 fibers per 1 cm (A-design, Russia). After application, samples were dried in a drying chamber at the temperature of 130°C and were subjected to high−temperature annealing in a HTC 40/16 furnace (Nabertherm, Germany) at the temperature of 1250°C for 2 h.

The morphology of composite powders before and after the series of reduction and oxidation cycles and also the microstructure of single crystal membranes and electrode layers were studied using a scanning election microscope (SEM) with a LEO Supra 50VP field emitting cathode. The device was equipped with an INCA Energy+ system of energy-dispersive X-ray microanalysis.

Thermogravimetric studies of composite anodic powders according to programs including a series of reduction and oxidation cycles at different temperatures were carried out using a Setaram Setsys EVO 16/18 thermogravimetric analyzer (Setaram, France) with modules of thermogravimetric analysis (TGA) and differential thermal analysis for studies of the temperature dependence of the mass and heat flux, accordingly. The device was equipped by a gas system with consumption controllers allowing to perform measurements in the atmosphere of oxygen, air, argon, technical mixture of argon and hydrogen (4% hydrogen), carbon dioxide, and also in vacuum.

Electrochemical studies of model SOFC were carried out using a gas−temperature test bench and a special sample holder described in detail in previous works [19, 20]. The model SOFC used were samples of the electrolyte−supporting structure based on ceramic solid electrolyte membranes of 8YSZ (92 mol % ZrO_2 + 8 mol % Y_2O_3) with the anodic electrode based on cermet of NiO/8YSZ = 40/60 wt % [21, 22] and also samples based on a single crystal membrane with the composition of 10Sc1YSZ and a two−layer anodic electrode consisting of functional (NiO/10Sc1CeSZ = 40/60 wt %) and current collector (NiO/10Sc1CeSZ = 60/40 wt %) sublayers.

RESULTS AND DISCUSSION

The anodic electrode of the manufactured samples was reduced at the temperature of 500°C in a mixture of hydrogen and nitrogen with the partial pressures of components being 0.5 atm. After this, it was oxidized in an air atmosphere at the temperature of 900°C. Reduction and oxidation were repeated three times. Evolution of the Raman spectrum obtained for the region at the anodic electrode−solid electrolyte interface was registered in the course of reduction. Fig. 2 shows the dependences of the intensity of the 615 cm^{-1} band on time for three cycles of reduction of the anodic electrode.

The initial high intensity level is related to the process stage when the Raman spectrum corresponds to nickel oxide, while the final low level corresponds to complete reduction of nickel oxide to the metal state. As seen in Fig. 2, the first reduction cycle fundamentally differs from the two following ones. Both the initial delay before the reduction process and the overall process rate differ significantly for the first dependence. The initial delay for the first reduction is much greater (0.2 h as compared to 0.05 h for the second reduction) and the overall process duration is high (about 0.1 h as compared with 0.05 h for the second and third ones). It was suggested that both these changes were related to significant changes in the morphology of nickel oxide particles comprising the anodic electrode of model SOFC.

To test this assumption, composite powders of similar composition subjected to the same program of reduction and oxidation cycles in the thermogravimetric analyzer chamber were manufactured. Powders were
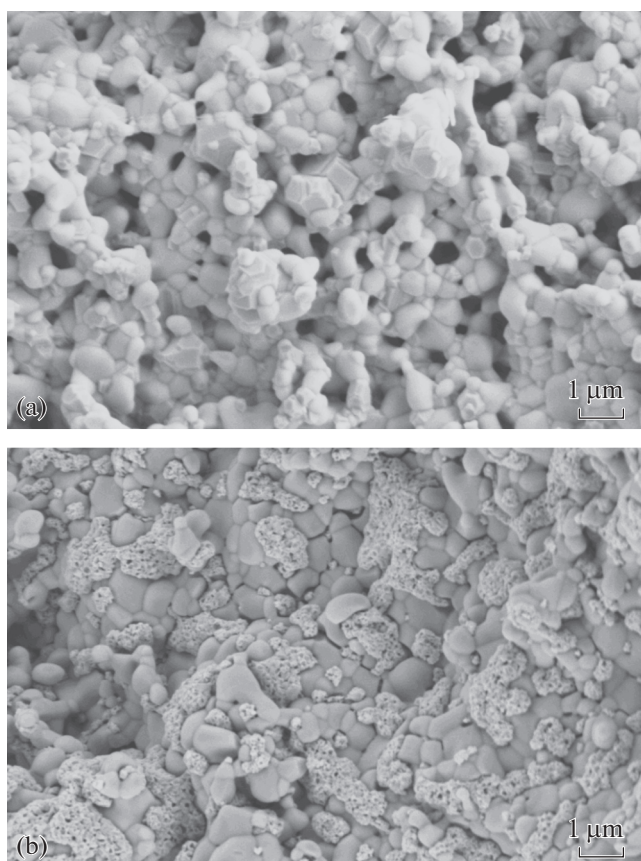
Fig. 3. SEM images of composite anode powder (a) before and (b) after the series of reduction and oxidation cycles.

Fig. 4. SEM images of the anodic SOFC electrode in contact with the single crystal membrane of solid electrolyte after a series of reduction and oxidation cycles.

Fig. 5. Results of thermogravimetric analysis of composite anodic powder as dependent on the reduction cycle number.

studied using the scanning electron microscopy method. The initial and final images are shown in Fig. 3.

As seen in Figs. 3a and 3b, the sizes of NiO and 10Sc1CeSZ grains in the initial powder are comparable and are about 0.3−0.5 μm. After a series of reduction and oxidation cycles, the size of the solid electrolyte particles remained unchanged and the size of nickel oxide particles, in its turn, decreased significantly to the value of about 50−100 nm.

The SEM image (Fig. 4) of the SOFC anode electrode after electrochemical tests combined with studies using the Raman scattering technique confirm the assumption regarding the mechanism of the decrease in the reduction time.

As seen in Fig. 4, the size of nickel oxide grains within the composite anode is much lower than the size of grains of the 10Sc1CeSZ solid electrolyte, though grains of comparable size were used in the manufacturing of the composite powder.

Similar studies of redox cycling were carried out using composite powder in a thermogravimetric analyzer chamber. The dependences of the mass on the time for the first three reduction cycles are shown in Fig. 5.
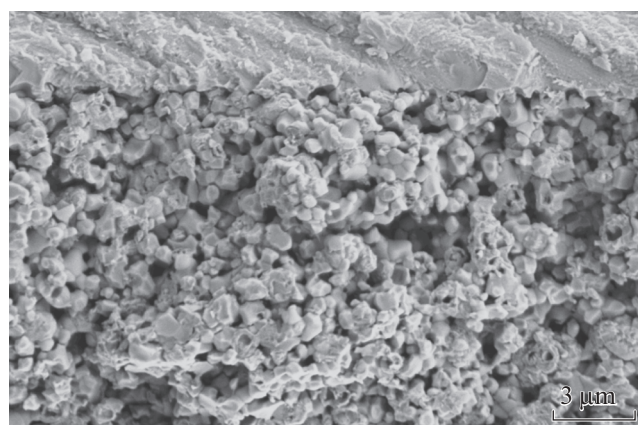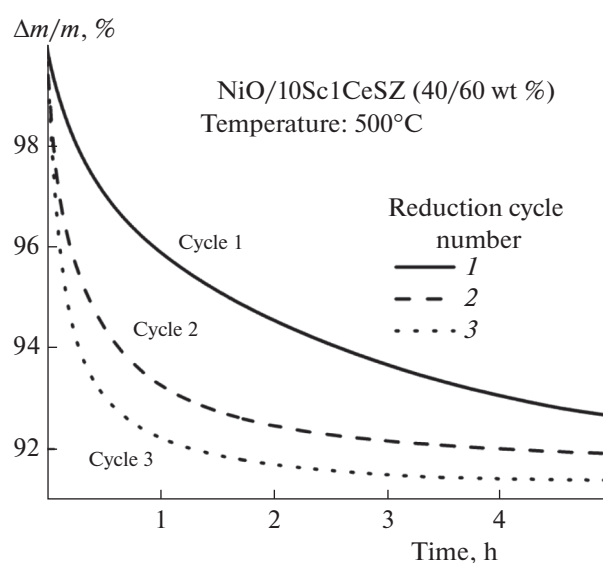
As seen in the presented dependences, the TGA technique qualitatively confirms the results of studies using the Raman scattering technique. The first reduction occurs in a much longer time than the further ones. However, one should point out that the process in measurements using Raman spectroscopy occupies about 0.05 h for the second and further cycles, while its duration in the studies using the Raman scattering technique is at least 2−3 h.

Qualitatively, the reduction process is shown in the case of studies using the Raman spectroscopy and thermogravimetric analysis techniques of the powder in Fig. 6.

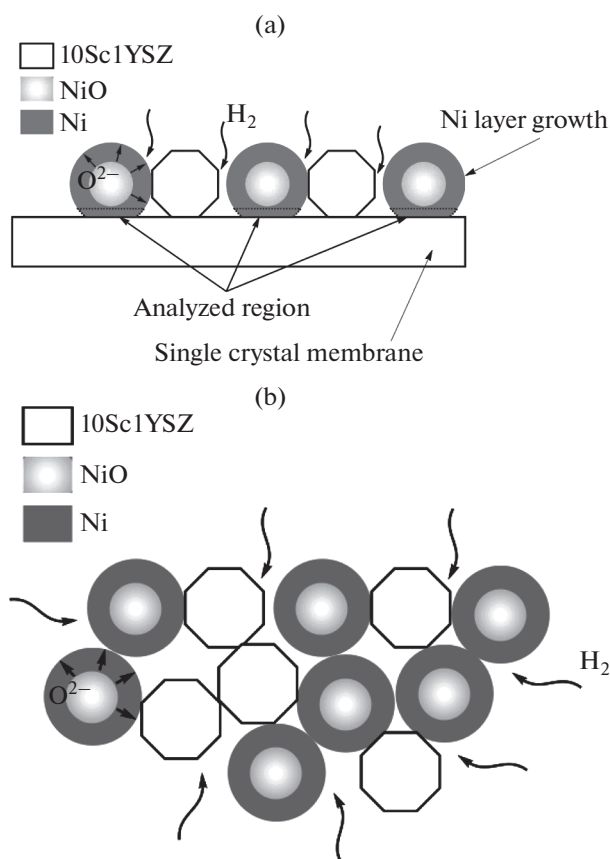When Raman spectroscopy is used, the signal is registered in the narrow region of the anodic elec-

Fig. 6. Schematic image of the process of reduction of the composite SOFC anode in studies using (a) the Raman scattering technique and (b) thermogravimetric analysis.

Fig. 7. (a) Dependence of voltage on model SOFC during the initial reduction of composite single crystal anode electrode and (b) dependences of voltage for the first and second reduction cycles.

trode−electrolyte interface. This is the cause of the delay observed in all the intensity−time dependences: it is required for the reduction front to reach the outer electrode boundary, the anode−electrolyte interface. From the same viewpoint, it appears possible to explain the different time required for occurrence of the whole reduction cycle. The complete reduction process is studied in the case of using thermogravimetric analysis, while the Raman spectroscopy technique is used to investigate reduction of only a small boundary area that requires much less time for the reduction cycle.

Fig. 7a shows the dependences of voltage on model SOFC on time for the case of the initial cell reduction at the temperature of 900°C, while Fig. 7b demonstrates the dependences of voltage for the first and second cycles of the anodic electrode reduction.

As seen in Fig. 7a, the first reduction cycle can take considerable time; the voltage exceeds the level of 1.1 V in 1−2 h at the temperature of 900°C. At a transition to medium−temperature SOFC, the duration of initial reduction increases considerably due to the slowing of the kinetics of nickel oxide reduction.
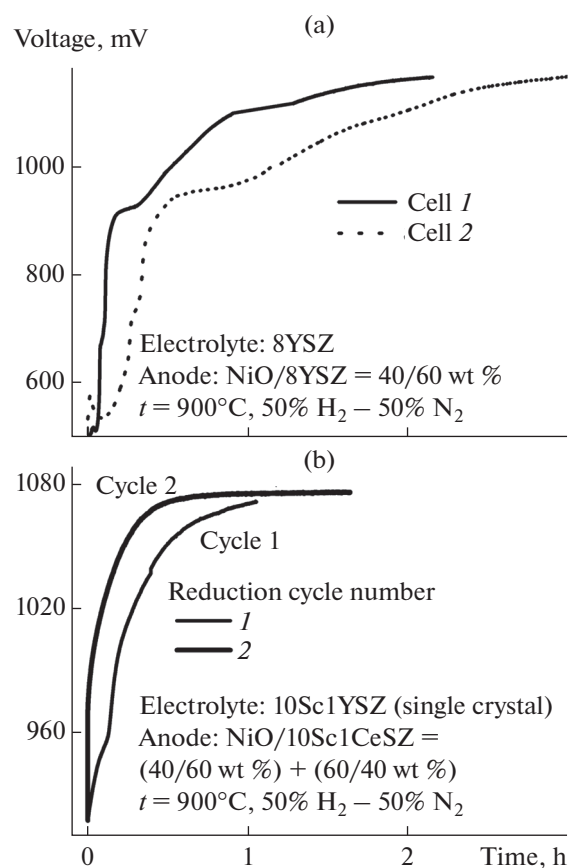
As seen from the dependences shown in Fig. 7b, the kinetics of the anodic electrode reduction depends considerably on the reduction cycle number. In the first cycle, overcoming the level of 1.05 V requires about 0.5 h while in the second cycle the duration is about 0.25 h. Thus, the results of studies of the kinetics of nickel oxide reduction can be used for optimization of the initial mode of reduction of the SOFC anodic electrode.

CONCLUSIONS

The work studies the kinetics of reduction and morphological changes of nickel grains in composite SOFC anodes. It is shown in studies using the Raman spectroscopy and thermogravimetric analysis techniques that the first reduction cycle differs considerably from the further cycles both with respect to the initial delay and the overall process duration. Studies using the SEM method show that these changes are related to the fundamental morphological restructuring occurring in the course of the first reduction cycle: the size of nickel oxide grains decreases considerably as compared to the initial size.

The general scheme of the process in the studies of model cells using the Raman spectroscopy technique and also in the case of thermogravimetric analysis of powders shows the causes for the significant difference between the overall process time obtained by different techniques.

The results of studies of the kinetics of nickel oxide reduction within SOFC composite anodes can be used for optimization of the mode of initial reduction of the anodic electrode when the model medium—temperature SOFC reach the operating conditions.

ACKNOWLEDGMENTS

REFERENCES

1. Wachsman, E.D. and Lee, K.T., *Science,* 2011, vol. 334, p. 935.
2. Huijsman, J.P.P., van Berkel, F.P.F., and Christie, G.M., *J. Power Sources,* 1998, vol. 71, p. 107.
3. Dusastre, V. and Kilner, J.A., *Solid State Ionics,* 1999, vol. 126, p. 163.
4. Fu, C., Sun, K., Zhang, N., Chen, X., and Zhou, D., *Electrochim. Acta,* 2007, vol. 52, p. 4589.
5. Nielsen, J., Jacobsen, T., and Wandel, M., *Electrochim. Acta,* 2011, vol. 56, p. 7963.
6. Rembelski, D., Viricelle, J.P., Combemale, L., and Rieu, M., *Fuel Cells,* 2012, vol. 12, p. 256.
7. Hecht, E.S., Gupta, G.K., Zhu, H., Dean, A.M., Kee, R.J., Maier, L., and Deutschmann, O., *Appl. Catal., A,* 2005, vol. 295, p. 40.
8. Lee, J.-H., Moon, H., Lee, H.-W., Kim, J., Kim, J.-D., and Yoon, K.-H., *Solid State Ionics,* 2002, vol. 148, p. 15.
9. Koide, H., Someya, Y., Yoshida, T., and Maruyama, T., *Solid State Ionics,* 2000, vol. 132, p. 253.
10. Ishihara, T., Yan, J., Shinagawa, M., and Matsumoto, H., *Electrochim. Acta,* 2006, vol. 52, p. 1645.
11. Ju, Y.-W., Eto, H., Inagaki, T., Ida, S., and Ishihara, T., *J. Power Sources,* 2010, vol. 195, p. 6294.
12. Ju, Y.-W., Ida, S., Inagaki, T., and Ishihara, T., *J. Power Sources,* 2011, vol. 196, p. 6062.
13. Agarkov, D.A., Burmistrov, I.N., Tsybrov, F.M., Tartakovskii, I.I., Kharton, V.V., Bredikhin, S.I., and Kveder, V.V., *ECS Trans.,* 2015, vol. 68, p. 2093.
14. Borik, M.A., Lomonova, E.E., Osiko, V.V., Panov, V.A., Porodnikov, O.E., Vishnyakova, M.A., and Koron'ko, Yu.K., *J. Cryst. Growth,* vol. 275, no. h. 2005.
15. Aleksandrov, V.I., Osiko, V.V., Prokhorov, A.M., and Tatarintsev, V.M., *Russ. Chem. Rev.,* 1978, vol. 47, p. 213.
16. Artemov, V.G., Kuritsyna, I.E., Lebedev, S.P., Komandin, G.A., Karpalov, P.O., Spektor, I.E., Kharton, V.V., Bredikhin, S.I., and Volkov, A.A., *Russ. J. Electrochem.,* 2014, vol. 50, p. 690.
17. Burmistrov, I., Agarkov, D., Bredikhin, S., Nepochatov, Yu., Tiunova, O., and Zadorozhnaya, O., *ECS Trans.,* 2013, vol. 57, p. 917.
18. Burmistrov, I.N., Agarkov, D.A., Tartakovskii, I.I., Kharton, V.V., and Bredikhin, S.I., *ECS Trans.,* 2015, vol. 68, p. 1265.
19. Agarkov, D.A., *M. Sc. Dissertation,* Chernogolovka: IFTT RAN, 2013.
20. Burmistrov, I.N., *Cand. Sci. (Phys.—Math.) Dissertation,* Chernogolovka: IFTT RAN, 2011.
21. Burmistrov, I., Drozhzhin, O., Istomin, S., Sinitsyn, V., Antipov, E., and Bredikhin, S., *J. Electrochem. Soc.,* 2009, vol. 156, p. B1212.
22. Burmistrov, I. and Bredikhin, S., *ECS Trans.,* 2009, vol. 25, p. 2793.

Translated by M. Ehrenburg

SPELL: 1. ok